

Short-time behavior of the diffusion coefficient as a geometrical probe of porous media

Partha P. Mitra

*Schlumberger-Doll Research, Old Quarry Road, Ridgefield, Connecticut 06877-4108
and Department of Physics, Harvard University, Cambridge, Massachusetts 02138*

Pabitra N. Sen and Lawrence M. Schwartz

*Schlumberger-Doll Research, Old Quarry Road, Ridgefield, Connecticut 06877-4108
(Received 17 November 1992)*

We investigate the time-dependent diffusion coefficient, $D(t) = \langle r^2(t) \rangle / (6t)$, of random walkers in porous media with piecewise-smooth pore-grain interfaces. $D(t)$ is measured in pulsed-field-gradient spin-echo (PFGSE) experiments on fluid-saturated porous media. For reflecting boundary conditions at the interface we show that for short times $D(t)/D_0 = 1 - A_0(D_0t)^{1/2} + B_0D_0t + O[(D_0t)^{3/2}]$, where $A_0 = 4S/(9\sqrt{\pi}V_p)$ and $B_0 = -HS/(12V_p) - \sum_i(L_i/V_p)f(\phi_i)$. Here D_0 is the diffusion constant of the bulk fluid, S/V_p is the surface area to pore volume ratio, H is the mean curvature of the smooth portions of the surface, L_i is the length of a wedge of angle ϕ_i , and the function $f(\phi)$ is defined below. More generally, we consider partially absorbing boundary conditions, where the absorption strength is controlled by a surface-relaxivity parameter ρ . Here, the density of walkers (i.e., the net magnetization) decays as $M(t) = 1 - \rho St/V_p + \dots$, and $D(t)$ is defined as $\langle r^2(t) \rangle_s / (6t)$, where $\langle r^2(t) \rangle_s$ is the mean-square displacement of surviving walkers. When $\rho \neq 0$ we find that the coefficient A_0 of the $\sqrt{D_0t}$ term in the above equation is *unchanged*, while the coefficient of the linear term changes to $B_0 + \rho S/(6V_p)$. Thus, data on $D(t)$ and $M(t)$ at short times may be used *simultaneously* to determine S/V_p and ρ . The limiting behavior of $D(t)$ as $\rho \rightarrow \infty$ is also discussed.

I. INTRODUCTION

The ratio of surface area to pore volume, S/V_p , is an important parameter describing the microgeometry of porous media, and is a key factor governing numerous physical processes such as catalysis, electrolytic conduction in systems with charged interfaces, and nuclear magnetic resonance (NMR).¹⁻⁴ Recently, we described a method of determining S/V_p using the time-dependent diffusion coefficient of fluid molecules in fluid-saturated porous media as measured by the pulsed-field-gradient spin-echo (PFGSE) technique.⁵ PFGSE experiments measure the diffusion of nuclear magnetization in fluids which arises, physically, out of the diffusive motion of the fluid molecules.^{6,7} The magnetization density can be visualized as the density of an ensemble of random walkers moving through the pore space and getting either reflected or absorbed at the pore-grain interface.⁷⁻¹⁰ Physically, the absorption of walkers reflects the enhanced relaxation of magnetization associated with paramagnetic impurities at the grain surfaces.³ Let $\langle r^2(t) \rangle_s$ be the mean-square displacement of the walkers surviving to time t . We derive a perturbation expansion for the time-dependent diffusion coefficient, $D(t) \equiv \langle r^2(t) \rangle_s / (6t)$, at short times. Successive terms in the perturbation series contain integer powers of the diffusion length $(D_0t)^{1/2}$. The first term of this expansion was exploited successfully by Latour *et al.*¹¹ to determine S/V_p in a number of experimental systems.

We make the observation, important in the context of PFGSE experiments, that the coefficient of the $(D_0t)^{1/2}$ term (in the expansion described above) is *unaltered* by

the presence of enhanced surface relaxation. Thus the (generally unknown) surface-relaxivity parameter ρ does *not* enter the determination of S/V_p . By contrast, traditional methods of measuring S/V_p using NMR are based on the fact that the decay rate of the net magnetization, $M(t)$, is enhanced by an amount $\rho(S/V_p)$.³ The utility of this method is clearly limited by the fact that the value of ρ is required to determine S/V_p . The present results suggest a method of determining ρ and S/V_p together by combining measurements of the short-time behavior of $M(t)$ and $D(t)$. We believe this to be the only reliable way of determining S/V_p values relevant to NMR measurements in fluid-saturated porous media.⁴ The widely used Brunauer-Emmett-Teller (BET) method suffers from several drawbacks in that it generally employs gas molecules interacting with a dry pore-grain interface.¹² NMR, however, is sensitive to the wetted surface area which can be very different from the dry surface area, especially when expandable clays are present. Further, the surface area determined by the BET method often depends on the size of the gas molecule used and the dead volume in the instruments can introduce additional uncertainty.¹²

We wish to emphasize that the results derived here hold as well for early-time diffusion coefficients determined by other methods, such as light-scattering experiments on macromolecules in porous media.¹³ This is true because the underlying diffusion equations and the boundary conditions are identical. The time-dependent PFGSE amplitude $M(\mathbf{k}, t)$ corresponds to the intermediate scattering function in light-scattering experiments. In addition, $M(\mathbf{k}=\mathbf{0}, t)$ corresponds to the heat flux in a

thermal-diffusion problem or to the solute concentration in catalysis or electrochemistry problems.¹⁴

The study of the short-time transients of the diffusion equation in restricted geometries has a long and colorful history which is described in a classic paper by Kac entitled "Can one hear the shape of a drum?,"¹⁵ More recent citations are given in Ref. 14 which deals with mass and heat transfer problems. Kac considered the problem of determining the geometry of the boundary from the spectral function

$$\theta(t) = \sum_{n=1}^{\infty} \exp(-\lambda_n t), \quad (1)$$

where $\{\lambda_n\}$ are the eigenvalues of the diffusion equation in a region surrounded by perfectly absorbing walls. More recently, de Gennes discussed an analogous problem related to the decay of magnetization, $M(t)$, in a region where the relaxation rate at the boundary is infinite.¹⁶ The present study involves the diffusion coefficient $D(t)$, which is related to the second moment of displacement. We will see that $M(t)$ and $D(t)$ involve information about both the eigenfunctions and eigenvalues of the diffusion equation.

This paper is organized as follows: In Sec. II we summarize how $D(t)$ is measured in PFG experiments and present a simple physical picture for the early-time behavior of $D(t)$. Section II concludes with the derivation of a perturbative expansion for the diffusion propagator. In Sec. III we consider in detail the early-time behavior of $D(t)$. Beginning with reflecting boundary conditions, we treat first smooth interfaces and then wedgelike singularities. The influence of partially absorbing boundary conditions is then included. An illustrative example, diffusion within an isolated spherical pore, is presented in Sec. IV. In Sec. V we describe the results of numerical simulations on model two- and three-dimensional pore geometries. An alternate derivation of the influence of surface relaxation using an eigenfunction expansion is given in the Appendix.

Because the formalism developed below is somewhat complex, this section concludes with a brief summary of our principal results. In a porous medium with a pore surface which is smooth except for wedge-shaped regions where the curvature is allowed to be singular, and with a finite surface relaxivity ρ , one has

$$M(t) = 1 - \rho t S / V_p + O(t^{3/2}), \quad (2a)$$

$$D(t)/D_0 = 1 - A \sqrt{D_0 t} + B D_0 t + O(t^{3/2}), \quad (2b)$$

where

$$A = \frac{4S}{9V_p \sqrt{\pi}} \quad (3)$$

and

$$B = -\frac{1}{12} H \frac{S}{V_p} + \frac{1}{6} \frac{\rho S}{D_0 V_p} - \sum_i \frac{L_i}{V_p} f(\phi_i), \quad (4)$$

where H is the mean curvature averaged over the smooth parts of the surface,

$$H = \frac{1}{S} \int d\sigma \left[\frac{1}{R_1} + \frac{1}{R_2} \right]. \quad (5)$$

Here R_1 and R_2 are the principal radii of curvature at each point on the interface and L_i is the length of the i th wedge with angle ϕ_i . The function $f(\phi)$ is given in a later section. As ρ becomes larger, the crossover time, after which terms higher order in ρ become important, becomes shorter, until at $\rho = \infty$, the leading square-root term changes and gets a new coefficient. At $\rho = \infty$, we show that

$$M(t) = 1 - (2\sqrt{D_0 t S}) / (\sqrt{\pi} V_p) + O(t), \quad (6a)$$

$$D(t)/D_0 = 1 - A_1 \sqrt{D_0 t} + B_1 D_0 t + O(t^{3/2}), \quad (6b)$$

where

$$A_1 = \frac{2S}{9V_p \sqrt{\pi}} \quad (7)$$

and

$$B_1 = -\frac{1}{6} H \frac{S}{V_p} - \sum_i \frac{L_i}{V_p} f_1(\phi_i). \quad (8)$$

Thus the coefficient of the $\sqrt{D_0 t}$ term in $D(t)$ changes only by a factor of 2 when ρ changes from a finite value to infinity. The methods developed in Sec. III A 2 could be used to derive an explicit representation for the function $f_1(\phi)$. However, because the $\rho \rightarrow \infty$ limit is of little experimental interest, we have not completed this calculation.

II. GENERAL CONSIDERATIONS

A. Pulsed-field-gradient spin-echo measurements

In PFGSE measurements, the spin-echo radio frequency pulse sequence is combined with the application of two gradient pulses, each of which, briefly, imposes a spatial dependence on the static magnetic field (Fig. 1). We make the simplifying assumptions $\delta \rightarrow 0$, and $g \rightarrow \infty$ such that the gradient-pulse strength δg remains constant. We also assume that all transverse evolution times approach zero. In this limit we can neglect (1) diffusion while the magnetization is in the transverse plane and (2) the effects of spatial randomness in the local Larmor frequency. Physically, the two gradient pulses act to dephase and then rephase the spins involved in the underlying spin-echo measurement. In the absence of diffusion the effects of these two pulses cancel exactly. However, if a spin originally at \mathbf{r} diffuses to \mathbf{r}' at time t , its net phase change is $\gamma \delta \mathbf{g} \cdot (\mathbf{r} - \mathbf{r}')$, where γ is the gyromagnetic ratio. The wave vector $\mathbf{k} \equiv \gamma \delta \mathbf{g}$ is then a tunable parameter and the spin-echo amplitude is given by⁷

$$M(\mathbf{k}, t) = \frac{1}{V_p} \int \int d\mathbf{r} d\mathbf{r}' G(\mathbf{r}, \mathbf{r}', t) e^{-i\mathbf{k} \cdot (\mathbf{r} - \mathbf{r}')}. \quad (9)$$

The propagator $G(\mathbf{r}, \mathbf{r}', t)$ satisfies the diffusion equation in the interior of the pore space,

$$\frac{\partial G(\mathbf{r}, \mathbf{r}', t)}{\partial t} = D_0 \nabla^2 G(\mathbf{r}, \mathbf{r}', t), \quad t > 0, \quad (10)$$

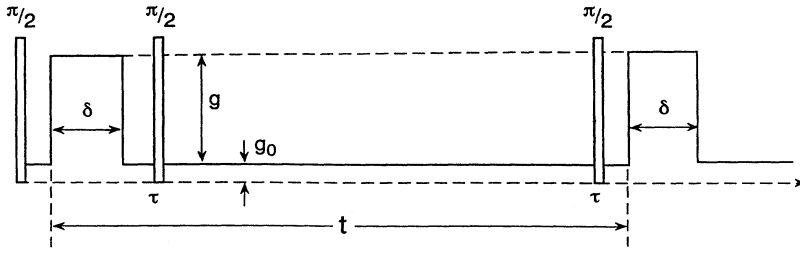


FIG. 1. Tanner stimulated pulse-echo sequence (Ref. 6). Here the radio frequency pulses are of duration τ , the field-gradient pulses are of duration δ , g_0 is a constant background gradient, and $\delta g \gg \tau g_0$.

subject to the initial condition $G(\mathbf{r}, \mathbf{r}', t=0^+) = \delta(\mathbf{r} - \mathbf{r}')$. The boundary condition at the pore-grain interface Σ is

$$D_0 \hat{\mathbf{n}} \cdot \nabla G(\mathbf{r}, \mathbf{r}', t) + \rho G(\mathbf{r}, \mathbf{r}', t)|_{\mathbf{r} \in \Sigma} = 0, \quad (11)$$

where $\hat{\mathbf{n}}$ denotes the outward (i.e., into the grain) normal. In isotropic porous media the PFGSE experiment operationally defines a time-dependent diffusion coefficient through the relation

$$-\lim_{k \rightarrow 0} \frac{\partial \ln[M(k, t)]}{\partial k^2} = \frac{\langle r^2(t) \rangle_s}{6} \equiv D(t)t. \quad (12)$$

More generally, the diffusion coefficient is a symmetric 3×3 tensor.

B. Physical arguments

In the *absence* of surface relaxation, the random walkers simply bounce off the interface Σ , their number being conserved. Under these familiar conditions, the equation $D(t) = \langle r^2(t) \rangle / (6t)$ provides a natural definition of the time-dependent diffusion constant. In absence of the interface, $D(t) = D_0$, the diffusion constant of the bulk fluid. With the interface restricting the motion of the walkers, $D(t)$ decreases in time from its initial value D_0 . At early times, assuming a piecewise-smooth interface, only walkers within a diffusion length $(D_0 t)^{1/2}$ sense the presence of the reflecting boundary. Since only the fraction $(D_0 t)^{1/2} S / V_p$ has sensed the boundary, the diffusion coefficient starts decaying as

$$D(t) = D_0(t) [1 - \alpha (D_0 t)^{1/2} S / V_p + O(D_0 t)], \quad (13)$$

where α is a numerical constant. If the diffusion is not anomalous at long times, then $D(t)$ saturates to an asymptotic value, $\lim_{t \rightarrow \infty} D(t) = D_\infty$ which is related to the *electrical* conductivity σ of the fluid-saturated network,

$$\frac{\phi D_\infty}{D_0} = \frac{\sigma}{\sigma_f}, \quad (14)$$

where σ_f is the conductivity of the bulk pore fluid.¹⁷

In the presence of surface relaxation, the number of random walkers is not conserved, so that the motion of the walkers is no longer diffusive in the usual sense. However, the PFGSE measurement still provides a time-dependent diffusion coefficient via the operational definition (12). We consider the rms displacement $\langle r^2(t) \rangle_s$ averaged over only those walkers *surviving* to time t and define $D(t)$ as $\langle r^2(t) \rangle_s / (6t)$. As a concrete,

but trivial, example, consider random walkers moving in free space, but in the presence of a uniform density of sinks; here the number of walkers decays exponentially in time, but the surviving walkers move the same distance that they would have without the sinks. Accordingly, in this simple case, we have $D(t) = D_0$. If the distribution of sinks is not uniform, $D(t)$ no longer equals D_0 . However, we note the remarkable fact that the presence of a finite surface relaxation has no *effect* on the leading term in Eq. (13). This can be crudely understood in terms of a simple dimensional argument, at least for smooth surfaces. We will show below [Eq. (20)] that, for smooth boundaries, there is a perturbation expansion of the propagator, with successive terms containing positive integer powers of the surface area S and surface relaxivity ρ . At early times, the deviation of $D(t)/D_0$ from 1 should be proportional to S/V_p . Since $D(t)/D_0$ is dimensionless, we have to multiply S/V_p by a length to obtain this deviation. When $\rho = 0$, to the lowest orders in time, this length is clearly given as $(D_0 t)^{1/2} + D_0 t/R + O(t^{3/2})$, where R is some other geometric length scale in the system, such as the mean radius of curvature. When ρ is nonzero but finite, to the same order in time, the only other length we can construct is ρt . (Note that ρ has the dimensions of velocity, and we are allowed only positive integer powers of ρ .) Thus the deviation in $D(t)/D_0$ can be written as $\alpha (D_0 t)^{1/2} S / V_p + \beta (\rho + D_0/R) t + O(t^{3/2})$ (where β is a numerical coefficient), so that the leading term in $(D_0 t)^{1/2}$ is manifestly unaffected.

C. Perturbative expansion for the propagator

In this section we derive a perturbative expansion of the propagator that is good at short times, and use this expansion in the following section to derive the short-time expansion of the diffusion coefficient expansion at short times. It follows from Eq. (10) that the Laplace transform $\tilde{G}(\mathbf{r}, \mathbf{r}', s)$ of the Green's function satisfies the equation

$$s \tilde{G}(\mathbf{r}, \mathbf{r}', s) - \delta(\mathbf{r} - \mathbf{r}') = D_0 \nabla^2 \tilde{G}(\mathbf{r}, \mathbf{r}', s). \quad (15)$$

The boundary conditions are also Laplace transformed, to give

$$D_0 \hat{\mathbf{n}} \cdot \nabla \tilde{G}(\mathbf{r}, \mathbf{r}', s) + \rho \tilde{G}(\mathbf{r}, \mathbf{r}', s)|_{\mathbf{r} \in \Sigma} = 0. \quad (16)$$

Let $\tilde{G}_0(\mathbf{r}', \mathbf{r}'', s)$ be any other function that satisfies the diffusion equation in the pore space, i.e.,

$$s \tilde{G}_0(\mathbf{r}', \mathbf{r}'', s) - \delta(\mathbf{r}' - \mathbf{r}'') = D_0 \nabla^2 \tilde{G}_0(\mathbf{r}', \mathbf{r}'', s). \quad (17)$$

Multiplying (15) by $\tilde{G}_0(\mathbf{r}', \mathbf{r}'', s)$, (17) by $\tilde{G}(\mathbf{r}, \mathbf{r}', s)$, integrating over \mathbf{r}' , and subtracting, we obtain

$$\begin{aligned} \tilde{G}(\mathbf{r}, \mathbf{r}'', s) &= \tilde{G}_0(\mathbf{r}, \mathbf{r}'', s) \\ &+ D_0 \int d\mathbf{r}' [\tilde{G}_0(\mathbf{r}', \mathbf{r}'', s) \nabla'^2 \tilde{G}(\mathbf{r}, \mathbf{r}', s) \\ &- \tilde{G}(\mathbf{r}, \mathbf{r}', s) \nabla'^2 \tilde{G}_0(\mathbf{r}', \mathbf{r}'', s)] . \end{aligned} \quad (18)$$

Converting the volume integrals to surface integrals, and using the boundary condition (16), we obtain

$$\begin{aligned} \tilde{G}(\mathbf{r}, \mathbf{r}'', s) &= \tilde{G}_0(\mathbf{r}, \mathbf{r}'', s) \\ &- D_0 \int d\sigma' \tilde{G}(\mathbf{r}, \mathbf{r}', s) \\ &\times \left[\hat{\mathbf{n}}' \cdot \nabla' + \frac{\rho}{D_0} \right] \tilde{G}_0(\mathbf{r}', \mathbf{r}'', s) . \end{aligned} \quad (19)$$

Direct iteration of the integral equation (19) leads to a series expansion for \tilde{G} . The expansion is valid at large s , corresponding to short times. The first two terms in the expansion are

$$\begin{aligned} \tilde{G}(\mathbf{r}, \mathbf{r}'', s) &= \tilde{G}_0(\mathbf{r}, \mathbf{r}'', s) \\ &- D_0 \int d\sigma' \tilde{G}_0(\mathbf{r}, \mathbf{r}', s) \\ &\times \left[\hat{\mathbf{n}}' \cdot \nabla' + \frac{\rho}{D_0} \right] \tilde{G}_0(\mathbf{r}', \mathbf{r}'', s) \\ &+ \dots . \end{aligned} \quad (20)$$

For an appropriate of $\tilde{G}_0(\mathbf{r}, \mathbf{r}', s)$, Eq. (20) yields a perturbation series in integer powers of $\sqrt{D_0/s}$.

III. SHORT-TIME EXPANSION

A. Reflecting boundary conditions

1. Smooth interfaces

The short-time expansion of the diffusion constant may be easily derived with the help of the equation of motion satisfied by the mean-square displacement $R^2(t) = (1/V_p) \int d\mathbf{r} d\mathbf{r}' (\mathbf{r} - \mathbf{r}')^2 G(\mathbf{r}, \mathbf{r}', t)$. Working in the Laplace representation, this definition, together with Eqs.

(10) and (11), leads to

$$s\tilde{R}^2(s) = \frac{6D_0}{s} - 2D_0 \int \frac{d\mathbf{r}'}{V_p} \int d\sigma \tilde{G}(\mathbf{r}, \mathbf{r}', s) (\mathbf{r} - \mathbf{r}') \cdot \hat{\mathbf{n}} . \quad (21)$$

The second term on the right-hand side of (21) consists of a surface integral over the point \mathbf{r} and a volume integral over the point \mathbf{r}' . At large s , corresponding to short times, the integrand is exponentially small unless \mathbf{r}' is within a diffusion length $\sqrt{D_0/s}$ of \mathbf{r} . Thus, for fixed \mathbf{r} , only the region of the surface within a diffusion length of the surface need be taken into account. Let us first assume that the surface is smooth in a small neighborhood of the point \mathbf{r} . At the shortest times, the surface may be approximated by the tangent plane at \mathbf{r} . Using the short-time expansion (20), we shall take G_0 to be the propagator satisfying reflecting boundary conditions at the tangent plane at \mathbf{r} . It will be convenient to hold \mathbf{r} fixed and perform the integral over \mathbf{r}' in (21). To do this, we set up a coordinate system with the origin at \mathbf{r} and the positive z axis along the inward surface normal. If the x and y axes are chosen to lie along the principle directions of (interface) curvature, then, close to the origin, the surface is described by the equation

$$z = \frac{1}{2} \left[\frac{x^2}{R_1} + \frac{y^2}{R_2} \right] + \dots , \quad (22)$$

where R_1, R_2 are the principle radii of curvatures at \mathbf{r} .¹⁴ The geometry is illustrated in Fig. 2. In this coordinate system, \tilde{G}_0 is given by

$$\tilde{G}_0(\mathbf{r}', \mathbf{r}'', s) = \frac{1}{4\pi D_0} \left[\frac{e^{-(s/D_0)^{1/2} r_1}}{r_1} + \frac{e^{-(s/D_0)^{1/2} r_2}}{r_2} \right] , \quad (23)$$

where

$$r_1 = \sqrt{(x' - x'')^2 + (y' - y'')^2 + (z' - z'')^2} \quad (24a)$$

and

$$r_2 = \sqrt{(x' - x'')^2 + (y' - y'')^2 + (z' + z'')^2} . \quad (24b)$$

Substituting the expansion (20) with $\rho=0$ into Eq. (21), we get

$$s\tilde{R}^2(s) = \frac{6D_0}{s} - \frac{2D_0}{V_p} \int d\mathbf{r}' \int d\sigma (\mathbf{r} - \mathbf{r}') \cdot \hat{\mathbf{n}} \left[\tilde{G}_0(\mathbf{r}, \mathbf{r}', s) - \int d\sigma'' \tilde{G}_0(\mathbf{r}, \mathbf{r}'', s) \hat{\mathbf{n}}'' \cdot \nabla'' \tilde{G}_0(\mathbf{r}'', \mathbf{r}', s) \right] . \quad (25)$$

Let us look in detail at the first integral on the right-hand side of (25); reversing the orders of integration we have

$$- \frac{2D_0}{V_p} \int d\sigma \int d\mathbf{r}' (\mathbf{r} - \mathbf{r}') \cdot \hat{\mathbf{n}} \tilde{G}_0(\mathbf{r}, \mathbf{r}', s) . \quad (26)$$

Since $\tilde{G}_0(\mathbf{r}, \mathbf{r}', s)$ falls off exponentially when $|\mathbf{r} - \mathbf{r}'| \gg \sqrt{D_0/s}$, and since $\sqrt{D_0/s}$ is very small, the interface can be replaced by the surface (22). Thus, in the \mathbf{r}' integration, the variable z' ranges from

$z'(x', y') = 1/2(x'^2/R_1 + y'^2/R_2)$ to $z' = \infty$. Integrating over \mathbf{r}' using the coordinate system pictured in Fig. 2, we have

$$\begin{aligned} &\int d\mathbf{r}' (\mathbf{r} - \mathbf{r}') \cdot \hat{\mathbf{n}} \tilde{G}_0(\mathbf{r}, \mathbf{r}', s) \\ &\approx \frac{\epsilon^3}{2\pi D_0} \int_{-\infty}^{\infty} dx_0 dy_0 \int_{z_0(x_0, y_0)}^{\infty} dz_0 \frac{e^{-r_0}}{r_0} \\ &= \frac{\epsilon^3}{D_0} + O(\epsilon^5) . \end{aligned} \quad (27)$$

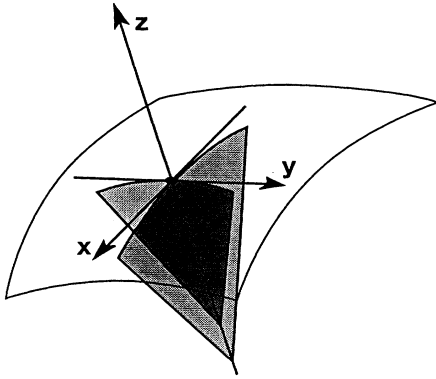


FIG. 2. Principal radii of curvature are indicated (by the shaded circle segments) for a typical surface element. Also shown is the coordinate system employed in Sec. III A 1.

Here the diffusion length $\epsilon = \sqrt{D_0/s}$ has been used to scale the integration variables. In the rescaled coordinate system, $z_0(x_0, y_0) = \epsilon/[2(x_0^2/R_1 + y_0^2/R_2)]$. Also, $\int_{z_0(x_0, y_0)}^{\infty} dz_0 \equiv \int_0^{\infty} dz_0 - \int_0^{z_0(x_0, y_0)} dz_0$. In the last step of (27) we have expanded the integral in powers of ϵ , noting that $z_0(x_0, y_0)$ is of order ϵ when x_0, y_0 are of order one. (When x_0, y_0 are much larger than 1, the integrands are exponentially small.) Thus, for the integral (26), we obtain $2S/V_P(D_0/s)^{3/2} + O((D_0/s)^{5/2})$. The second integral (25) can be worked out in an analogous manner and we have

$$s\bar{R}^2(s) = \frac{6D_0}{s} - \frac{S}{V_P} \left[2 \left(\frac{D_0}{s} \right)^{3/2} + \left(\frac{D_0}{s} \right)^2 \left\langle \frac{1}{R_1} + \frac{1}{R_2} \right\rangle \right] + O((D_0/s)^{5/2}), \quad (28)$$

where $\langle \dots \rangle \equiv S^{-1} \int d\sigma(\dots)$. Taking the Laplace transform of (28), the leading terms in the early-time expansion for $D(t)$ are

$$D(t) = D_0 \left[1 - \frac{S}{V_P} \frac{4}{9\sqrt{\pi}} (D_0 t)^{1/2} - \frac{1}{12} (D_0 t) \left\langle \frac{1}{R_1} + \frac{1}{R_2} \right\rangle \right] + O((D_0 t)^{3/2}). \quad (29)$$

It is interesting to note that for reflecting smooth walls, the sign of the linear term in $D(t)$ is that of the average curvature. This can be intuitively understood as follows: First, for a flat surface, the linear term is absent. If the surface is slightly concave, e.g., in the interior of a sphere, the walker is somewhat more restricted at short times than it would be by a flat wall. Thus, the effect of a positive curvature is to decrease $D(t)$ even more than its leading $\sqrt{D_0 t}$ correction. This crude argument gives the right sign of the linear term.

2. Effects of wedges

To derive the effect of a wedge, we return to (21). Consider a wedge of angle ϕ and length L . We shall neglect

effects coming from the boundaries of the wedge. Let us set up the coordinate system, so that the z axis is along the axis of the wedge, and the x axis is along one of the sides. Motion in the z direction is free and decouples from the x - y motion. Because the time domain propagator factorizes [i.e., $G(\mathbf{r}_1, \mathbf{r}_2, t) = G(\rho_1, \rho_2; t)G_0(z_1, z_2, t)$, where $\rho_1 = \{x_1, y_1\}$ and $\rho_2 = \{x_2, y_2\}$], we can integrate over z before performing the Laplace transform,

$$s\bar{R}^2(s) = \frac{6D_0}{s} - 2D_0 \frac{L}{V_P} \times \int d\rho_2 \int d\sigma_1 \tilde{G}(\rho_1, \rho_2, s) (\rho_1 - \rho_2) \cdot \hat{\mathbf{n}}_1, \quad (30)$$

where $\tilde{G}(\rho_1, \rho_2, s)$ is now a two-dimensional Green's function. Now the Green's function for a wedge of internal angle ϕ in two dimensions is known¹⁴ in terms of a Kontorovich-Lebedev transformation (which is essentially a Fourier transform for the radial variable). We rescale variables so that lengths are measured in terms of the diffusion length $\sqrt{D_0/s}$. For reflecting boundary conditions the rescaled propagator is given by

$$G(\rho_1, \rho_2; \phi_<, \phi_>) = \frac{2}{\pi^2} \int_0^{\infty} dx K_{ix}(\rho_1) K_{ix}(\rho_2) \times \cosh[x\phi_<] \cosh[x(\phi_> - \phi)] \frac{\sinh[\pi x]}{\sinh[\phi x]}. \quad (31)$$

Using this form of the Green's function, we find that the integral in (30) is divergent; however, a finite answer can be obtained by subtracting the value at $\phi = \pi$ (corresponding to a flat surface, for which contribution has already been calculated). Finally, after a Laplace transform, the result is

$$D(t) = D_0 \left[1 - \frac{S}{V_P} \frac{4}{9\sqrt{\pi}} (D_0 t)^{1/2} - \frac{L}{3V_P} (D_0 t) f(\phi) \right] + O((D_0 t)^{3/2}), \quad (32)$$

where $f(\phi) = g(\phi) - g(\pi)$, $g(\phi)$ being given by

$$g(\phi) = \int_0^{\infty} dx \tanh \left[\frac{\pi x}{2} \right] \frac{\cosh(\phi x) - \cos(\phi)}{\sinh(\phi x)}. \quad (33)$$

The function $F(\phi)$ is plotted in Fig. 3. An amusing feature of this result is that the wedge correction *vanishes* for $\phi = \pi/2$. The function $f(\phi)$, shown in Fig. 3, changes sign at $\pi/2$, and the correction from an acute wedge actually increases $D(t)$ over its flat surface value. It is as if the walkers near an acute wedge are effectively pushed out of the corner by repeated bouncing off the walls.

B. Partially absorbing boundary conditions

In this section we show that for finite surface relaxivity ρ , the coefficient A of the $\sqrt{D_0 t}$ term in Eq. (2b) remains *unchanged*, and the coefficient of the linear term changes

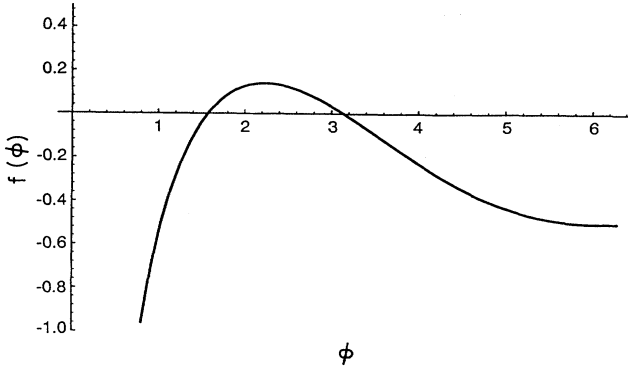


FIG. 3. Function $f(\phi)$ that describes the angular dependence of the wedge contribution to the term linear in $D_0 t$. (The horizontal axis is measured in radians.)

to $B = B(\rho=0) + \rho S / (6V_P)$. Thus, a finite ρ does not affect the leading short-time behavior of $D(t)$. The density of the walkers starts decaying as $M(t) = 1 - \rho S t / V_P + O(t^{3/2})$. This means that the data at short times on $D(t)$ and $M(t)$ can be combined to determine ρ and S/V_P , two important parameters governing NMR relaxation in porous media.

By our earlier definition (12),

$$6tD(t) = \frac{\langle [\mathbf{r}(t) - \mathbf{r}'(0)]^2 \rangle_{\text{un}}}{M(0,t)} = \frac{1}{V_P M(0,t)} \int d\mathbf{r} d\mathbf{r}' G(\mathbf{r}, \mathbf{r}', t) (\mathbf{r} - \mathbf{r}')^2, \quad (34)$$

where the subscript “un” denotes un-normalized expectation value. The evaluation of the short-time diffusion coefficient is facilitated by considering the equation of motion ($t > 0$),

$$\frac{\partial \langle [\mathbf{r}(t) - \mathbf{r}'(0)]^2 \rangle_{\text{un}}}{\partial t} = \frac{D_0}{V_P} \int d\mathbf{r} d\mathbf{r}' (\mathbf{r} - \mathbf{r}')^2 \nabla^2 G(\mathbf{r}, \mathbf{r}', t). \quad (35)$$

Integrating by parts, we have

$$\begin{aligned} \frac{\partial \langle [\mathbf{r}(t) - \mathbf{r}'(0)]^2 \rangle_{\text{un}}}{\partial t} &= \frac{D_0}{V_P} \int d\mathbf{r}' d\mathbf{s} \cdot \nabla G(\mathbf{r}, \mathbf{r}', t) (\mathbf{r} - \mathbf{r}')^2 \\ &\quad - 2 \frac{D_0}{V_P} \int d\mathbf{r}' d\mathbf{s} \cdot (\mathbf{r} - \mathbf{r}') G(\mathbf{r}, \mathbf{r}', t) \\ &\quad + 2dD_0 M(0,t). \end{aligned} \quad (36)$$

Now, consider a flat surface at which partially absorbing boundary conditions are imposed. This gives the lowest-order correction in ρ , which we will find is linear in time. Including effects of curvature as above produces only higher-order effects. We set up our coordinate system with the z axis lying along the surface normal. The Green's function is separable in this coordinate system, so that $G(\mathbf{r}, \mathbf{r}', t) = G_0(x, x', t) G_0(y, y', t) G(z, z', t)$. Since the z axis is along the surface normal, $G_0(y, y', t)$ and

$G_0(x, x', t)$ are free propagators [e.g., $G_0(x, x', t) = e^{-(x-x')^2/(4D_0 t)} (4\pi D_0 t)^{-1/2}$]. As above, we fix \mathbf{r} at the coordinate origin and carry out the integral over \mathbf{r}' :

$$\begin{aligned} s\tilde{R}_{\text{un}}^2(s) &= - \int_0^\infty dz' \left[\frac{\rho S}{V_P} \left[z'^2 - 4D_0 \frac{\partial}{\partial z'} \right] + \frac{2D_0 S}{V_P} z' \right] \\ &\quad \times \frac{e^{-\kappa z'}}{\kappa D_0 + \rho} + 2dD_0 \tilde{M}(s). \end{aligned} \quad (37)$$

Here $\kappa = \sqrt{s/D_0}$ and we have employed the Laplace representation of the one-dimensional Green's function for finite ρ ,

$$\tilde{G}(z_<, z_>, s) = \frac{e^{-\kappa z_>}}{\kappa D_0} \left[\frac{\kappa D_0 - \rho}{\kappa D_0 + \rho} e^{\kappa z_<} + e^{-\kappa z_<} \right]. \quad (38)$$

After performing the integration, we expand in powers of $\sqrt{D_0}/s$. Laplace transforming, and dividing throughout by $M(t) = 1 - \rho t S / V_P + O(t^{3/2})$, we have

$$\frac{D(t)}{D_0} = 1 - \frac{4\sqrt{D_0} t S}{9V_P \sqrt{\pi}} + \frac{\rho t S}{6V_P} + O((D_0 t)^{3/2}). \quad (39)$$

An alternate derivation of this result is given in the Appendix.

IV. ISOLATED SPHERICAL PORE

In this section exact results are presented for diffusion inside a sphere. These results provide a check on the general equations derived above. We use the eigenfunction expansion to compute the Green's function. In this case there is rotational symmetry about the direction of the field gradient and the eigenvalues and eigenfunctions are

$$\frac{1}{T_{ln}} = \frac{D_0 \xi_{ln}^2}{a^2}, \quad (40a)$$

$$\psi_{l,n} = N_{ln} j_l(\xi_{ln} r/a) Y_{l0}(\theta, \phi), \quad (40b)$$

where j_l are spherical Bessel functions of order l , Y_{lm} are spherical harmonics,⁷ N_{ln} is a normalization constant, and the root ξ_{ln} corresponds to the n th root of the equation

$$\xi_{ln} j_l'(\xi_{ln}) = - \frac{\rho a}{D_0} j_l(\xi_{ln}). \quad (41)$$

$M(k, t)$ is given by⁷

$$\begin{aligned} M(k, t) &= \sum_{ln=0}^{\infty} \frac{6(2l+1) \xi_{ln}^2 e^{-D_0 t \xi_{ln}^2 / a^2}}{(\xi_{ln}^2 - k^2 a^2)^2} \\ &\quad \times \frac{k a j_l'(ka) + \frac{\rho a}{D_0} j_l(ka)}{\left[\frac{\rho a}{D_0} - \frac{1}{2} \right]^2 + \xi_{ln}^2 - (l + \frac{1}{2})^2}. \end{aligned} \quad (42)$$

A. Reflecting boundary conditions

From the eigenfunction expansion of the propagator, we obtain

$$\begin{aligned} R^2(t) &\equiv 6tD(t) = \langle [\mathbf{r}(t) - \mathbf{r}'(0)]^2 \rangle \\ &= \frac{6}{5}a^2 - 12a^2 \sum_{n=1}^{\infty} \frac{e^{-D_0 \xi_{1n}^2 t/a^2}}{\xi_{1n}^2 (\xi_{1n}^2 - 2)}, \end{aligned} \quad (43)$$

where the eigenvalues are given by

$$\left. \frac{j_l(r \xi_{1n}/a)}{\partial r} \right|_{r=a} = 0. \quad (44)$$

These sums can be evaluated by transforming into the Laplace domain:

$$s\tilde{R}^2(s) = 12a^2 \sum_{n=1}^{\infty} \frac{1}{(\xi_{1n}^2 + sa^2/D_0)(\xi_{1n}^2 - 2)}. \quad (45)$$

Using the identity

$$\sum_{n=1}^{\infty} \frac{2x}{x^2 - \xi_{1n}^2} = \frac{j_1''(x)}{j_1'(x)}, \quad (46)$$

which can be established using the method of contour integration,¹⁸ we obtain a closed-form expression for $\tilde{R}^2(s)$. (Calculations based on the above equations are presented in Fig. 5 below.) To obtain the short-time behavior, we consider the large s expansion for $\tilde{R}^2(s)$ to obtain

$$\frac{D}{D_0} = 1 - \frac{4S}{9V_P} \left[\frac{D_0 t}{\pi} \right]^{1/2} - \frac{D_0}{2a^2} t + O(t^{3/2}). \quad (47)$$

B. Perfectly absorbing boundaries: $\rho = \infty$

The eigenvalues ξ_{ln} satisfy

$$j_l(\xi_{ln}) = 0. \quad (48)$$

The decay of total magnetization involves only $l=0$, since it is assumed that the initial magnetization is uniform, giving

$$M(t) = 6 \sum_{n=1}^{\infty} \frac{e^{-D_0 n^2 \pi^2 t/a^2}}{n^2 \pi^2}. \quad (49)$$

The un-normalized displacement squared average is given by

$$\begin{aligned} \langle [\mathbf{r}(t) - \mathbf{r}'(0)]^2 \rangle_{\text{un}} &= 12a^2 \sum_{n=1}^{\infty} \frac{e^{-D_0 n^2 \pi^2 t/a^2}}{n^4 \pi^4} (n^2 \pi^2 - 6) \\ &\quad - 12a^2 \sum_{n=1}^{\infty} \frac{e^{-D_0 \xi_{1n}^2 t/a^2}}{\xi_{1n}^2}. \end{aligned} \quad (50)$$

Again the Laplace transform of the above quantities can be evaluated in the closed form, and making a large s expansion, we obtain

$$M(t) = 1 - \frac{2S}{V_P} \left[\frac{D_0 t}{\pi} \right]^{1/2} + \frac{3D_0 t}{a^2} + O(t^{3/2}) \quad (51)$$

and

$$\frac{D}{D_0} = 1 - \frac{2S}{9V_P} \left[\frac{D_0 t}{\pi} \right]^{1/2} - \frac{D_0}{a^2} t + O(t^{3/2}). \quad (52)$$

V. DIFFUSION SIMULATIONS

To illustrate the utility of the analytic results derived in the preceding sections we have carried out random walk simulations of diffusion in a number of simple pore geometries. These simulations do not impose any fixed grid on the pore space; walkers move by taking steps of fixed length in a randomly chosen direction. At the pore-grain interface, either reflecting or partially absorbing boundary conditions are applied.⁸⁻¹⁰

We begin by considering a two-dimensional example based on an isosceles triangular pore with interior angles of $\pi/6$, $\pi/6$, and $2\pi/3$. The triangle's base length was

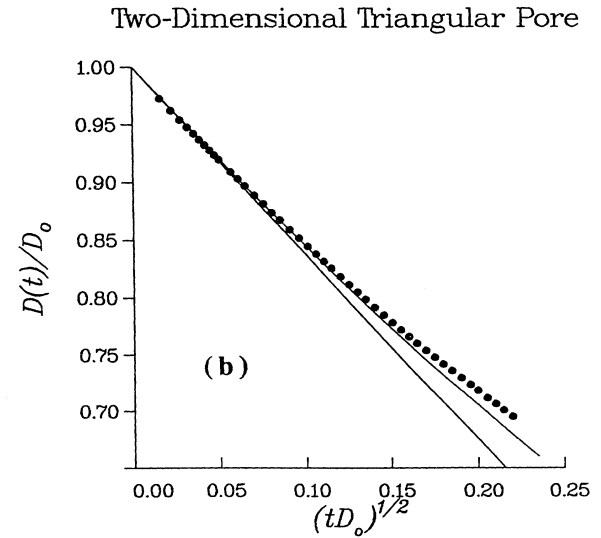
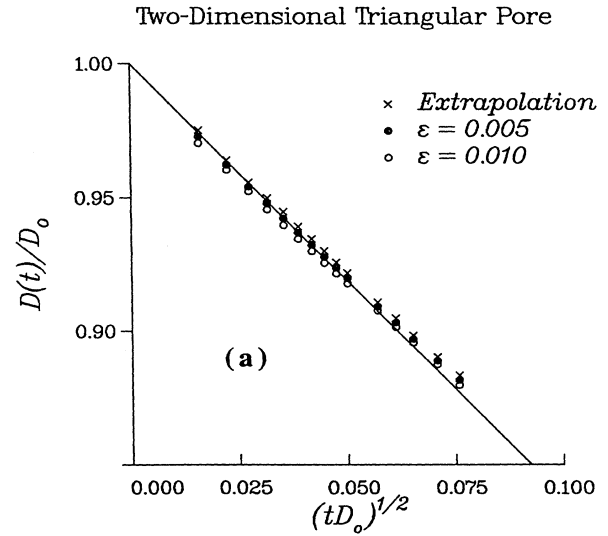


FIG. 4. Variation of $D(t)$ is shown for a two-dimensional isosceles triangular pore with internal angles of $\pi/6$, $\pi/6$, and $2\pi/3$. In (a) calculations based on two different random walk step sizes are compared with the results of a Richardson extrapolation. In (b) data for $\epsilon=0.005$ are compared with the linear and second-order corrections calculated in Sec. III A 2.

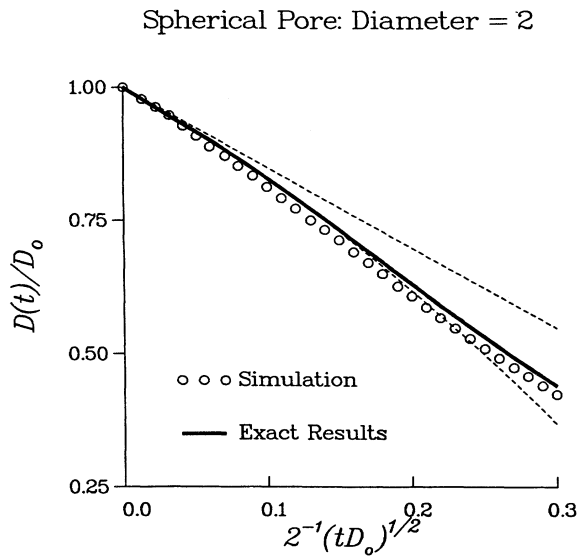


FIG. 5. Exact normal-mode calculations of $D(t)$ (thick curve) and numerical simulations (open circles) are compared for a spherical pore. Also shown (dashed curve) are the linear and second-order corrections calculated from the perturbation theory.

taken to be $2\sqrt{3}$, and its height was unity. Working with $\rho=0$, our interest is (1) to examine the influence of step size on the numerical data and (2) to illustrate the effects of the sharp angles on the behavior of $D(t)$ in accord with the results presented in Sec. III A 2. In Fig. 4(a) we compare, at very early times, the results of simulations carried out with two different step sizes with the leading-order correction of Eq. (32). For a given finite step size ϵ , the numerical data generally overestimate the decrease in

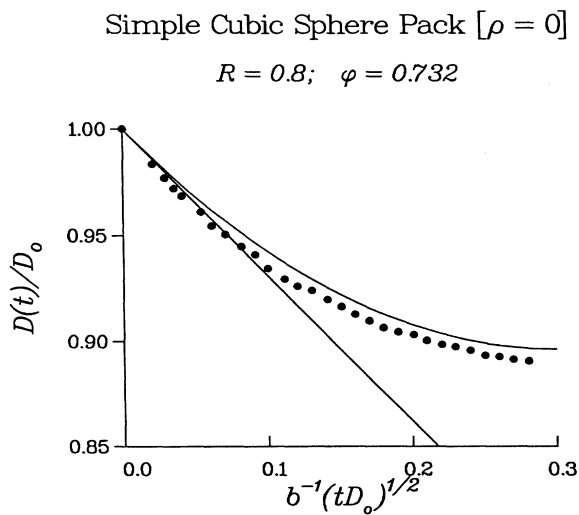


FIG. 6. Numerical simulations for a high-porosity simple cubic sphere pack are compared with the linear and second-order corrections calculated in perturbation theory. The difference between the simulations and the analytic results is due, in part, to finite step size effects.

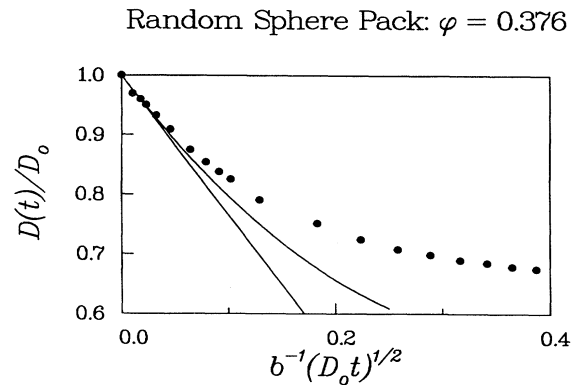


FIG. 7. Numerical simulations for a dense random sphere pack are compared with the linear and second-order corrections calculated in perturbation theory.

$D(t)$ because, for any ϵ , walkers with a distance ϵ of the interface can be influenced within a single time step. Shown in Fig. 4(a) are simulation results at the earliest times for two values of ϵ together with their Richardson extrapolation.¹⁹ The latter are seen to be in quite satisfactory agreement with the analytic estimate provided by the leading term of Eq. (32). From Fig. 4(b) we see that at somewhat later times the value of $D(t)/D_0$ moves above the $\sqrt{D_0 t}$ estimate in accord with the arguments given in Sec. III A 2. Shown also in this figure are the combined first- and second-order corrections. Generally the agreement between the simulations and the analytic results is quite satisfactory.

In Fig. 5 we consider the behavior of $D(t)$ for an isolated spherical pore. Here, our numerical simulations are

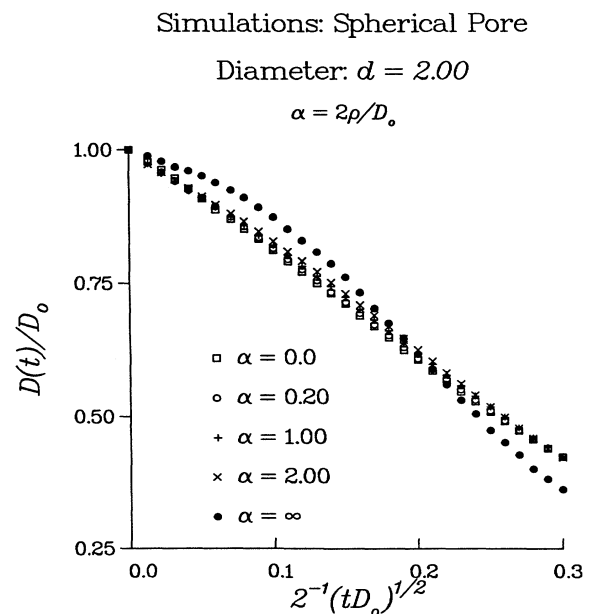


FIG. 8. Numerical simulations are presented for a spherical pore with various values of the surface relaxation parameter ρ . We note that the differences between the $\alpha=0.0, 0.20$, and 1.0 results are of the same order as the finite step size corrections.

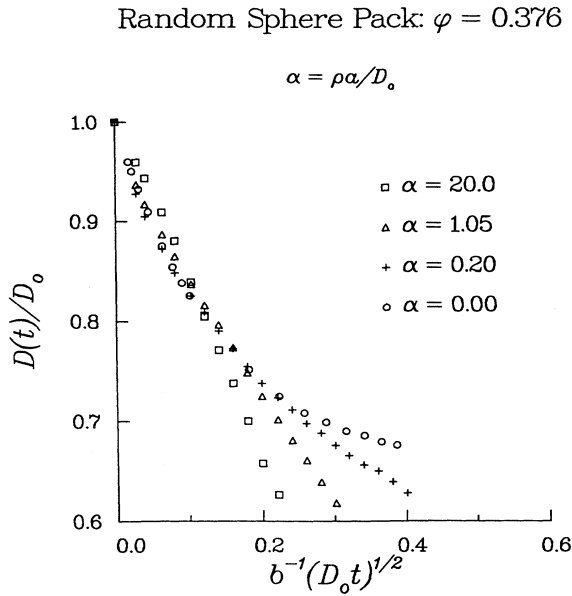


FIG. 9. Numerical simulations are presented for a dense random pack with various values of the surface relaxation parameter ρ .

compared with the exact results of Eq. (43) and with the leading terms of the expansion (47). (The fact that the simulation results lie below the solid curve is due to the finite size of the random walk steps.) A striking feature of these results is the fact that the first two terms of perturbation theory provide a reasonably accurate estimate of the diffusion coefficient up to the point where $D(t)$ has fallen to half of its original value, D_0 . Note that because the radii of curvature are equal and positive the coefficient of the term linear in $D_0 t$ is negative and the value of $D(t)$ drops below the lowest-order estimate. The opposite behavior is seen in Fig. 6. Here we consider diffusion in the interstitial region defined by a simple cubic packing of spherical grains. The sign of the principal radii is reversed and $D(t)/D_0$ data rise above the leading estimate as in Fig. 4. Qualitatively similar behavior is seen in Fig. 7 where we consider a dense random packing of nearly monodispersed spheres. (The grain radii were chosen from a uniform distribution whose half-width was 7.5% of its center position, in rough accord with the system studied experimentally by Latour *et al.*¹¹) These results are in excellent agreement with the data presented in Ref. 11. In the experiments of Latour *et al.* the measured lifetimes were long enough that the effects of enhanced surface relaxation can safely be neglected.

In Figs. 8 and 9 we consider the effects of the surface relaxation parameter ρ on the behavior of $D(t)/D_0$. In Fig. 8 we see that (in the spherical pore of Fig. 5) (1) as expected, the term proportional to $\sqrt{D_0 t}$ is not affected by ρ , and (2) the term proportional to $D_0 t$ is influenced only when ρ is large enough so that the first and second terms on the right-hand side of (4) are roughly comparable. For large values of ρ the sign of the $D_0 t$ term changes as predicted in Eq. (4). In Fig. 9 we see that, for the dense random sphere pack, the short-time behavior of

$D(t)/D_0$ is relatively unchanged by the introduction of weak surface relaxation. As we have already noted, the limit of large ρ appears not to be relevant to systems of experimental interest.

ACKNOWLEDGMENTS

We wish to thank R. Kleinberg and L. Latour for important conversations and suggestions. Conversations with P. Le Doussal, B. Halperin, D. Johnson, and W. Kenyon are also acknowledged. Work at Harvard was supported in part by National Science Foundation through the Harvard Materials Research Laboratory and Grant No. DMR-91-15491.

APPENDIX: METHOD OF PHASE SHIFTS FOR PARTIALLY ABSORBING BOUNDARY CONDITIONS

In this appendix, we provide an alternative derivation of the short-time expansion (39) for a flat surface $\rho \neq 0$. For $t \geq 0$, the Green's function can be written in terms of the eigenfunctions⁷

$$G(\mathbf{r}, \mathbf{r}', t) = \sum_{n=1}^{\infty} \psi_n(\mathbf{r}) \psi_n(\mathbf{r}') e^{-t/T_n}, \quad (\text{A1})$$

where $\psi_n(\mathbf{r})$ are the normalized eigenfunctions of the equations

$$D \nabla^2 \psi_n = -\frac{\psi_n}{T_n}, \quad D \hat{\mathbf{n}} \cdot \nabla \psi_n + \rho \psi_n|_{\mathbf{r} \in \Sigma} = 0. \quad (\text{A2})$$

For a flat wall, we need the one-dimensional propagator perpendicular to the wall. The appropriate eigenfunctions are

$$\Psi(q, x) = \frac{1}{\sqrt{4\pi}} (e^{iqx} + e^{2i\delta_q} e^{-iqx}), \quad (\text{A3})$$

where δ_q is chosen to satisfy the boundary conditions

$$\tan \delta_q = \frac{\rho}{D_0 q}, \quad (\text{A4})$$

which gives

$$G(z, z', t) = \int_{-\infty}^{+\infty} \frac{dq}{2\pi} e^{-D_0 q^2 t} \cos(qz - \delta_q) \cos(qz' - \delta_q). \quad (\text{A5})$$

This result is not presently available in the literature.

Now let us proceed to evaluate $M(k, t)$ using the above Green's function. The magnetization satisfies an equation of motion analogous to that for the diffusion coefficient. We assume that the times are short enough so that the surface (assumed to be smooth) can be replaced by a flat wall. Integrating over the directions parallel to the wall, and assuming that the normal to the wall is uniformly distributed, we obtain

$$\frac{\partial M(\mathbf{k}, t)}{\partial t} = -D_0 k^2 M(\mathbf{k}, t) - \frac{S}{2V_P} \int_{-1}^{+1} d\mu \int_0^\infty dx' \int_{-\infty}^{+\infty} \frac{dq}{2\pi} e^{-ikx'\mu(\rho - ikD_0\mu)} e^{-D_0 t [q^2 t + k^2(1-\mu^2)]} \cos \delta_q \cos(qx' - \delta_q),$$

where $\mu = \cos\theta$ with θ being the angle between \mathbf{k} and \hat{n} . For obtaining the short-time asymptotics, it is convenient to take the Laplace transform, which gives, after integrating over q and x' variables,

$$\tilde{M}(\mathbf{k}, s) = \frac{1}{s + D_0 k^2} \left[1 - \frac{S}{2V_P D_0} \int_{-1}^{+1} d\mu \frac{\rho \sqrt{s/D_0 + k^2(1-\mu^2)} - D_0 k^2 \mu^2}{[\sqrt{s/D_0 + k^2(1-\mu^2)} + \rho/D_0](s/D_0 + k^2)} \right]. \quad (\text{A6})$$

Note that the decay of total magnetization is obtained by setting $k=0$ in above and integrating over μ ,

$$\tilde{M}(\mathbf{k}=\mathbf{0}, s) = \frac{1}{s} - \frac{S}{2V_P} \frac{\rho}{s^{3/2}(\sqrt{s} + \rho/\sqrt{D_0})}. \quad (\text{A7})$$

Thus for $\rho \gg \sqrt{D_0/t}$, we find the short-time decay behavior as

$$M = 1 - 2 \frac{S}{V_P} \left[\frac{D_0 t}{\pi} \right]^{1/2} + \dots, \quad (\text{A8})$$

while for $\rho \ll \sqrt{D_0/t}$ we find the short-time decay behavior as

$$M = 1 - \frac{S}{V_P} \rho t + \dots. \quad (\text{A9})$$

Similarly, taking a derivative with respect to k^2 and set-

ting $k=0$ gives

$$L^{-1} \left[\frac{\partial \tilde{M}(\mathbf{k}, s)}{\partial k^2} \Big|_{k=0} \right] = -D(t) M(\mathbf{k}=\mathbf{0}, t), \quad (\text{A10})$$

where L^{-1} denotes the inverse Laplace transform. After much algebra, we obtain for $\rho \gg \sqrt{D_0/t}$, the short-time decay behavior

$$\frac{D(t)}{D_0} = 1 - \frac{2S}{9V_P} \left[\frac{D_0 t}{\pi} \right]^{1/2} + \dots, \quad (\text{A11})$$

while for $\rho \ll \sqrt{D_0/t}$ we find that the short-time diffusion coefficient decays as

$$\frac{D(t)}{D_0} = 1 - \frac{4S}{9V_P} \left[\frac{D_0 t}{\pi} \right]^{1/2} + \frac{S}{6V_P} \rho t + \dots. \quad (\text{A12})$$

¹Physics and Chemistry of Porous Media—11 (Schlumberger-Doll Research, October 15–17, 1986 in Ridgefield, Connecticut), Proceedings of the Second International Symposium on the Physics and Chemistry of Porous Media, edited by J. R. Banavar, J. Koplik, and K. W. Winkler, AIP Conf. Proc. No. 154 (AIP, New York, 1986).

²Physical Phenomena in Granular Materials, edited by G. D. Cody, T. H. Geballe, and P. Sheng, MRS Symposia Proceedings No. 195 (Materials Research Society, Pittsburgh, 1990).

³W. Kenyon, J. Howard, A. Sezginer, C. Straley, A. Matteson, K. Horkowitz, and R. E. Ehrlich, Trans. SPWLA Annu. Logging Symp. **30**, 1 (1989); K. R. Brownstein and C. E. Tarr, Phys. Rev. A **19**, 2446 (1979); D. O. SeEVERS, Trans. SPWLA Annu. Logging Symp. **7**, 1 (1966); C. H. Neuman and R. J. S. Brown, J. Pet. Technol. **62**, 2853 (1982); A. Timur, *ibid.* **21**, 775 (1969); R. J. S. Brown, Nature **189**, 388 (1961); J. D. Robinson and J. D. Loren, Soc. Pet. Eng. J. **249**, 268 (1970); R. L. Kleinberg and M. A. Horsfield, J. Magn. Res. **88**, 9 (1990).

⁴P. Debye, H. R. Anderson, Jr., and H. Brumberger, J. Appl. Phys. **28**, 679 (1957); P. N. Sen, C. Straley, W. E. Kenyon, and M. S. Whittingham, Geophysics **55**, 61 (1990); J. G. Berryman and S. C. Blair, J. Appl. Phys. **60**, 1930 (1986).

⁵P. P. Mitra, P. N. Sen, L. M. Schwartz, and P. LeDoussal, Phys. Rev. Lett. **68**, 3555 (1992).

⁶E. O. Stejskal, J. Chem. Phys. **43**, 3597 (1965); J. E. Tanner and E. O. Stejskal, *ibid.* **49**, 1768 (1968); P. T. Callaghan, Aust. J. Phys. **37**, 359 (1984); R. M. Cotts, Nature **351**, 467 (1991); P. T. Callaghan, D. MacGowan, K. J. Packer, and F. O. Zelaya, *ibid.* **351**, 467 (1991); J. Magn. Res. **90**, 177 (1990).

⁷P. P. Mitra and P. N. Sen, Phys. Rev. B **45**, 143 (1992).

⁸J. R. Banavar and L. M. Schwartz, Phys. Rev. Lett. **58**, 1411 (1987); C. Straley, A. Matteson, S. Feng, L. M. Schwartz, W. E. Kenyon, and J. R. Banavar, Appl. Phys. Lett. **51**, 1146 (1987); J. R. Banavar and L. M. Schwartz, in *Molecular Dynamics in Restricted Geometries*, edited by J. Klafter and J. M. Drake (Wiley, New York, 1989), p. 273.

⁹K. S. Mendelson, Phys. Rev. B **41**, 562 (1990).

¹⁰D. J. Wilkinson, D. L. Johnson, and L. M. Schwartz, Phys. Rev. B **44**, 4960 (1991).

¹¹L. L. Latour, P. P. Mitra, R. L. Kleinberg, and C. Sotak, J. Magn. Res. (to be published).

¹²D. Avnir, D. Farin, and P. Pfeifer, Nature **308**, 261 (1984).

¹³M. T. Bishop, Ph.D. thesis, University of Massachusetts, 1987.

¹⁴C. G. Phillips and K. M. Jansons, Proc. R. Soc. London A **428**, 431 (1990).

¹⁵M. Kac, Am. Math. Month. **73**, No. 4, 1 (1966).

¹⁶P. G. de Gennes, C. R. Acad. Sci. Paris **295**, 1061 (1982).

¹⁷L. M. Schwartz and J. R. Banavar, Phys. Rev. B **39**, 11965 (1989).

¹⁸G. N. Watson, *A Treatise on the Theory of Bessel Functions*, 2nd ed. (Cambridge University Press, Cambridge, England, 1980), Chap. 18.

¹⁹C. M. Bender and S. A. Orszag, *Advanced Mathematical Methods for Scientists and Engineers*, McGraw-Hill International Series in Pure and Applied Mathematics (McGraw-Hill, New York, 1978).